A New Type of Intermittency in an Electronic Circuit

Tomoji YAMADA, Kazuhiro FUKUSHIMA* and Taichi YAZAKI**

Division of Electronic Physics, Kyushu Institute of Technology
Kitakyushu 804
**Faculty of Education, Kumamoto University, Kumamoto 860*
***Department of Physics, Aichi University of Education, Kariya 448*

An intermittency which has a different origin from the Pomeau-Manneville types is studied in a coupled nonlinear LCR circuit. This type of intermittency has a close relation to the multiplicative noise process. The electronic circuit is made up of inductors, resistors and capacitor diodes. An experimental study is done in this system. The results are compared with those of a phenomenological theory based on the multiplicative noise process. Moreover, a numerical calculation is also carried out on the equations for the present circuit with observed nonlinear characteristics of diodes. Satisfactory agreement between the experimental and calculated results is obtained.

§ 1. Introduction

The intermittency mechanism has been studied as one of the routes to chaos from regular to periodic state.[1] The alternative occurrence of long laminer phases and short irregular bursts characterizes the intermittency. Near the intermittency threshold there appears a long time scale which is proportional to the inverse of the largest Lyapunov exponent. Three types of intermittencies are known with respect to the transition from periodic to chaotic state.[1]

Recently, we have found a different type of intermittency from Pomeau and Manneville's.[2] This type of intermittency exists in a system which shows a chaos-chaos transition phenomena. Near the chaos-chaos transition a certain dynamical variable shows an intermittent behavior. Typical systems which exibit this type of intermittency are classified into two groups and described by the differential equations. The first type is of a modulation system:

$$\frac{d\boldsymbol{r}}{dt}=\boldsymbol{F}(\boldsymbol{r},\boldsymbol{x};t)\,;\quad \boldsymbol{F}(0,\boldsymbol{x};t)=0\,,$$

$$\frac{d\boldsymbol{x}}{dt}=\boldsymbol{G}(\boldsymbol{x};t)\,, \tag{1·1}$$

where the dynamical variable $\boldsymbol{x}$ is assumed to behave chaotic and $\boldsymbol{r}$ shows an intermittency near the intermittency threshold. The second type is of a coupled chaos system[3] which is described in the form of the following differential equations for the dynamical variables $\boldsymbol{x}_1$ and $\boldsymbol{x}_2$:

$$\frac{d\boldsymbol{x}_1}{dt}=\boldsymbol{F}(\boldsymbol{x}_1;\, t)+(D/2)(\boldsymbol{x}_2-\boldsymbol{x}_1)\,,$$

$$\frac{d\boldsymbol{x}_2}{dt}=\boldsymbol{F}(\boldsymbol{x}_2;\, t)+(D/2)(\boldsymbol{x}_1-\boldsymbol{x}_2)\,, \tag{1·2}$$

where D is a coupling constant and the uncoupled system,

$$\frac{d\boldsymbol{x}}{dt}=\boldsymbol{F}(\boldsymbol{x};\, t)\,, \tag{1·3}$$

is assumed to be chaotic. In the system (1·2) the variable,

$$\boldsymbol{v}=\boldsymbol{x}_2-\boldsymbol{x}_1\,, \tag{1·4}$$

shows the intermittent behavior near the intermittent threshold. We have the corresponding mapping systems to Eqs. (1·1) and (1·2).[4]

The present intermittency has a close relation with the multiplicative noise model.[5] We can derive a reduced model for the systems (1·1) and (1·2). The reduced model has a form of the multiplicative noise model.[6] A main difference of the present intermittency from Pomeau and Manneville's is that there appears the distribution of burst amplitudes. On the other hand, in the Pomeau-Manneville intermittencies bursts have the same order of magnitude.

The purpose of the present paper is to study the coupled chaos system. Recently, a new trend in the field of chaotic dynamics is the study of spatiotemporal chaos.[7] In a spatiotemporal chaos the system behaves chaotically in space and time. The coupled system (1·2) can be considered as the simplest spatiotemporal chaos system which consists of two chaotic oscillators. In the present paper the study of the coupled chaos system is carried out in a nonlinear LCR circuit. The same types of systems have been often experimentally studied. For instance, the sequence of the period doubling bifurcation was studied by Linsay.[8] Type II intermittency was studied by Huang and Kim[9] and type III intermittency has been studied by the present authors.[10] In a coupled nonlinear electronic circuit, a measurement of $f(\alpha)$ spectrum was done to compare the results with those derived from the sine-circle map.[11] In these experiments a common feature is that the origin of nonlinearity comes from the nonlinear characteristics of diodes.

In §2 the multiplicative noise model is derived from the coupled chaos system and several formulae for averaged quantities are obtained from the model. In §3 we describe an experiment in a coupled nonlinear LCR circuit which consists of two subsystems connected with an inductor. Digital data are sampled by using an A/D converter. We show intermittent waveforms and calculate the averaged values to compare with the results derived from the multiplicative noise model. Numerical calculation on the equations for the present nonlinear circuit with observed characteristics of diodes is done in § 4. The final section is devoted to a summary and the discussion.

§ 2. Multiplicative noise model

We start with the following equations for the coupled chaos system which has a slightly extended form of Eq. (1·2):

$$\frac{d\boldsymbol{x}_1}{dt}=\boldsymbol{F}(\boldsymbol{x}_1;\,t)+(D/2)\{\boldsymbol{G}(\boldsymbol{x}_2)-\boldsymbol{G}(\boldsymbol{x}_1)\}\,,$$

$$\frac{d\boldsymbol{x}_2}{dt}=\boldsymbol{F}(\boldsymbol{x}_2;\,t)+(D/2)\{\boldsymbol{G}(\boldsymbol{x}_1)-\boldsymbol{G}(\boldsymbol{x}_2)\}\,, \tag{2·1}$$

where the D is a coupling constant and the uncoupled system, $\dot{\boldsymbol{x}}=\boldsymbol{F}(\boldsymbol{x};\,t)$, behaves chaotic. Introducing the quantity,

$$\bar{\boldsymbol{x}}=(\boldsymbol{x}_1+\boldsymbol{x}_2)/2\,, \tag{2·2}$$

we obtain the following equations up to the first order of the quantity $\boldsymbol{v}\equiv\boldsymbol{x}_2-\boldsymbol{x}_1$,

$$\frac{d\boldsymbol{v}}{dt}=\{\boldsymbol{F}'(\bar{\boldsymbol{x}};\,t)-D\boldsymbol{G}'(\bar{\boldsymbol{x}})\}\boldsymbol{v}\,,$$

$$\frac{d\bar{\boldsymbol{x}}}{dt}=\boldsymbol{F}(\bar{\boldsymbol{x}};\,t)\,, \tag{2·3}$$

where $\boldsymbol{F}'=(\partial\boldsymbol{F}/\partial\boldsymbol{x})_{\boldsymbol{x}=\bar{\boldsymbol{x}}}$ and $\boldsymbol{G}'=(\partial\boldsymbol{G}/\partial\boldsymbol{x})_{\boldsymbol{x}=\bar{\boldsymbol{x}}}$. The formal solution of Eq. (2·3) can be written as

$$\boldsymbol{v}(t)=U(t)\boldsymbol{v}(0) \tag{2·4}$$

with

$$U(t)=\exp_+\int_0^t\{\boldsymbol{F}'(\bar{\boldsymbol{x}};\,s)-D\boldsymbol{G}'(\bar{\boldsymbol{x}})\}ds\,, \tag{2·5}$$

where $\exp_+$ means the ordered exponential function. Now we define the matrix:

$$\Lambda=\lim_{t\to\infty}(1/t)\log U(t)\,. \tag{2·6}$$

For the uncoupled case $D=0$, the eigenvalues of the matrix Λ gives the Lyapunov spectrum for the system, $\dot{\boldsymbol{x}}=\boldsymbol{F}(\boldsymbol{x};\,t)$.

The largest eigenvalue λ_{m} of the matrix Λ determines the stability of the uniform state, $\boldsymbol{v}=0$. Namely, for $\lambda_{\mathrm{m}}<0$ the state $\boldsymbol{v}=0$ is stable, while for $\lambda_{\mathrm{m}}>0$ the magnitude of $\boldsymbol{v}$ increases as time goes on and the uniform state becomes unstable. For the special case (1·2) where $\boldsymbol{G}(\boldsymbol{x})=\boldsymbol{x}$, the λ_{m} can be written as

$$\lambda_{\mathrm{m}}=\lambda_{\mathrm{L}}-D\,, \tag{2·7}$$

where λ_{L} is the largest Lyapunov exponent for the uncoupled system. From Eq. (2·7) it can be seen that there exists a sharp transition point from the uniform state to the nonuniform state as the coupling constant D decreases. The threshold value of the transition is given by $D=\lambda_{\mathrm{L}}$.

Now we define the absolute value of $\boldsymbol{v}$ as

$$r(t)=|\boldsymbol{v}(t)|\,. \tag{2·8}$$

If we write $r(t)$ in the following form for sufficiently large t:

$$r(t)=\exp\{\lambda_m t+p(t)\}\,, \tag{2·9}$$

the quantity $p(t)$ should satisfy the equation:

$$\lim_{t\to\infty}(1/t)p(t)=0\,. \tag{2·10}$$

Equation (2·10) can be rewritten in the form:

$$\langle\xi(t)\rangle=0\,, \tag{2·11}$$

where $\xi(t)\equiv dp(t)/dt$ and $\langle\ \rangle$ denotes the time average. Thus, from Eq. (2·9) we get

$$\frac{d}{dt}\log r(t)=\lambda_m+\xi(t)\,. \tag{2·12}$$

The quantity $\xi(t)$ is assumed to be Gaussian white noise:[12]

$$\langle\xi(t)\xi(t')\rangle=Q\delta(t-t')\,. \tag{2·13}$$

The characteristic correlation time of $\xi(t)$ is of the order of the characteristic time of the quantity $\bar{\boldsymbol{x}}$. On the other hand, the characteristic time of r near the transition point is of the order of λ_m^{-1} and much longer than that of $\xi(t)$. This fact is the reason why the ξ behaves like a white noise. The Gaussian property is an assumption at the present stage. The effect of deviation from the Gaussian property is discussed in Ref. 12). When r becomes large for large t, a nonlinear term becomes important in the nonuniform state. By taking into account this fact, Eq. (2·12) can be written as

$$\frac{dr}{dt}=(\lambda_m-\beta r^n+\xi)r\,, \tag{2·14}$$

where we have added the nonlinear term βr^{n+1}. Equation (2·14) is of the same form as the multiplicative noise model.[5] The distribution function of r has a form of power law for small r and $\lambda_m>0$. For $\lambda_m<0$ the distribution function is of the form of δ-function centered at $r=0$.[5]

So far we have considered the coupled system consisting of two equivalent oscillating subsystems. However, we sometimes meet with the case where the coupled system is made up of nonequivalent subsystems. For example, the nonequivalence comes from the difference of the characteristics of diodes in the experiment of the coupled nonlinear LCR electronic circuit which will be considered in the next section. In order to consider this case, Eq. (2·1) is extended by replacing $\boldsymbol{F}(\boldsymbol{x}_i)$ and $\boldsymbol{G}(\boldsymbol{x}_i)$ with $\boldsymbol{F}_i(\boldsymbol{x}_i)$ and $\boldsymbol{G}_i(\boldsymbol{x}_i)$, respectively, where $i=1, 2$. If the strength of the nonequivalence is not large, we get in the lowest order approximation,

$$\frac{d\boldsymbol{v}}{dt}=H(\bar{\boldsymbol{x}};\,t)\boldsymbol{v}+I(\bar{\boldsymbol{x}};\,t)\,, \tag{2·15}$$

where

$$H=\boldsymbol{F}'(\bar{\boldsymbol{x}};\,t)-D\boldsymbol{G}'(\bar{\boldsymbol{x}}),$$

$$I=\Delta\boldsymbol{F}(\bar{\boldsymbol{x}};\,t)-D\Delta\boldsymbol{G}(\bar{\boldsymbol{x}}), \tag{2·16}$$

where $\boldsymbol{F}'=\partial\boldsymbol{F}/\partial\bar{\boldsymbol{x}}$, $\boldsymbol{G}'=\partial\boldsymbol{G}/\partial\bar{\boldsymbol{x}}$ with $\boldsymbol{F}=(\boldsymbol{F}_1+\boldsymbol{F}_2)/2$, $\boldsymbol{G}=(\boldsymbol{G}_1+\boldsymbol{G}_2)/2$ and $\Delta\boldsymbol{F}=\boldsymbol{F}_2-\boldsymbol{F}_1$, $\Delta\boldsymbol{G}=\boldsymbol{G}_2-\boldsymbol{G}_1$. The second term of Eq. (2·15) represents the effect of the nonequivalence of the subsystems. By comparing Eq. (2·15) with the first equation of (2·3), it can be seen that the effect of the nonequivalence plays a role of an external force in the equation of $\boldsymbol{v}$. The external force is important when the magnitude of $\boldsymbol{v}$, namely r, becomes small. Therefore, the first effect of the nonequivalence is to introduce a lower cutoff to the power law form of the distribution function derived in the case of the equivalent coupled oscillator system. The second effect of the nonequivalence is a role of an external additive force. Because of the existence of this external additive force, the distribution function or r takes a finite value even for $\lambda_m<0$. After all the distribution function $P(r)$ can be written as

$$P(r)=Cr^{-1+\eta} \tag{2·17}$$

for $r_0<r<r_c$ with $\eta=2\lambda_m/Q$. Here the lower cutoff r_0 and the upper cutoff r_c come from the effect of the nonequivalence of the subsystems and the existence of the nonlinear term, respectively. Namely, the distribution function for the r has the form of the power law in the region, $r_0<r<r_c$. The value of $P(r)$ rapidly goes to zero as r becomes larger than r_c.

By using Eq. (2·17) we can calculate the following averaged values:

$$\langle r\rangle=r_c f(1+\eta)/f(\eta) \tag{2·18}$$

and

$$\langle r^2\rangle=r_c^2 f(2+\eta)/f(\eta), \tag{2·19}$$

where

$$f(a)=\int_\varepsilon^1 dx x^{a-1}=(1-\varepsilon^a)/a \tag{2·20}$$

with $\varepsilon=r_0/r_c$.

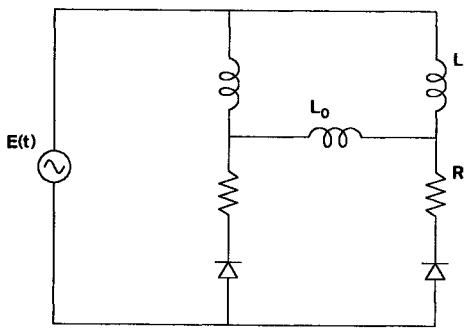

Fig. 1. Electronic circuit consisting of two coupled oscillating subsystems.

§ 3. Experiment in coupled nonlinear LCR circuit

The electronic circuit in which the present experiment is carried out is almost the same as used in Ref. 10) and shown in Fig. 1. The system consists of two oscillating subsystems, each of which is made up of an inductor L, a resistor R and a diode connected in series with a common electric source $E(t)$ where the values are taken as, $R=17.5\,\Omega$ and $L=100\,\mu$H. The two diodes

used in the present experiment are the varicaps (NEC1SV50) and are made to have similar nonlinear characteristics. The external voltage has the following form:

$$E(t)=V_b+G\cdot\sin(\omega t) \tag{3·1}$$

with $V_b=1$ V, $G=7$ V and $f=\omega/2\pi=2.75$ MHz. As shown in Ref. 10), for these parameters the uncoupled oscillating subsystems behave chaotic. The inductor L_0 connects the two subsystems and the value of L_0 is varied by preparing nine coils with different turns. The basic equations for the present circuit is given as follows:[10]

$$\begin{aligned} &L\cdot\frac{di_1}{dt}+\kappa(v_1+Ri_1-v_2-Ri_2)+Ri_1+v_1=E(t)\,,\\ &L\cdot\frac{di_2}{dt}+\kappa(v_2+Ri_2-v_1-Ri_1)+Ri_2+v_2=E(t)\,, \end{aligned} \tag{3·2}$$

where i_k and v_k $(k=1, 2)$ denote the currents through the resistors R and the voltages across the diodes, respectively, where the subscripts 1, 2 distinguish the two subsystems. Equation (3·2) can be considered as a special case of Eq. (2·1). The coupling

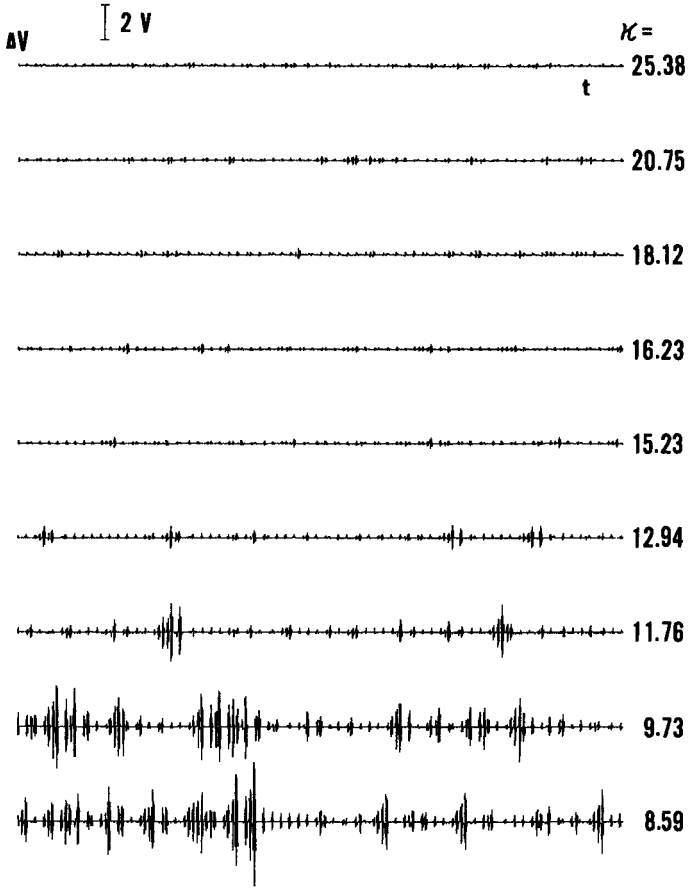

Fig. 2. The voltage difference ΔV between two diodes in the experiment. The horizontal axis t denotes the time.

constant κ is

$$\kappa = L/L_0 . \tag{3·3}$$

In Fig. 2 the voltage difference $\Delta V = v_2 - v_1$ between two diodes are displayed for different coupling constants κ. The data are sampled by the A/D converter (HITACHI VC-6165). In each figure the total time interval is 50 μs. The waveforms in Fig. 2 show strong intermittency as κ is decreased. The peculiar feature of the present intermittency is that the amplitudes of bursts are distributed. In Fig. 3 the distribution function of the $r \equiv |\Delta V|$ is illustrated for $\kappa = 11.76$, where 40000 data points digitized in units of 20/255 V are used. The log-log plots of the data points are on a single straight line in the intermediate range of r. This feature agrees with the multiplicative noise model explained in § 2. The exponent η for the distribution function $P(r)$ is defined through $P(r) \propto r^{-1+\eta}$. The values η for different κ can be obtained and are shown in Fig. 4. The full line denotes the following straight line:

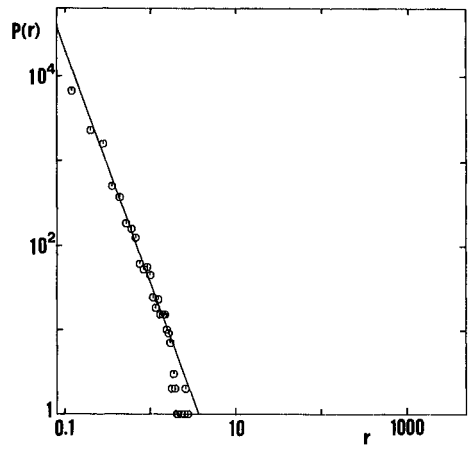

Fig. 3. The distribution function $P(r)$ of the quantity $r \equiv |\Delta V|$ for $\kappa = 11.76$ obtained in the experiment.

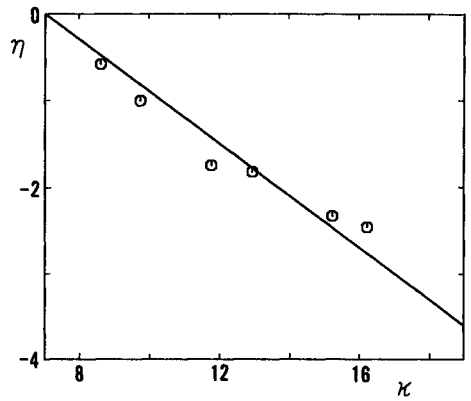

Fig. 4. The exponent η for the distribution function $P(r)$ obtained in the experiment.

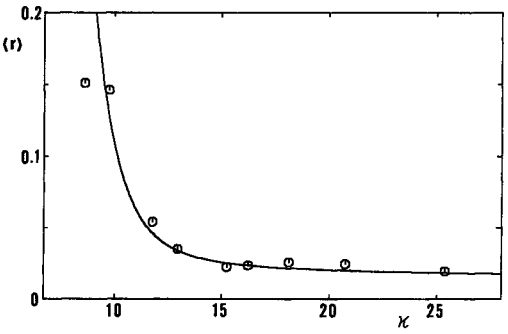

Fig. 5. The averaged value $\langle r \rangle$ in the experiment. The circles denote the experimental data and the full line is of the theoretical curve.

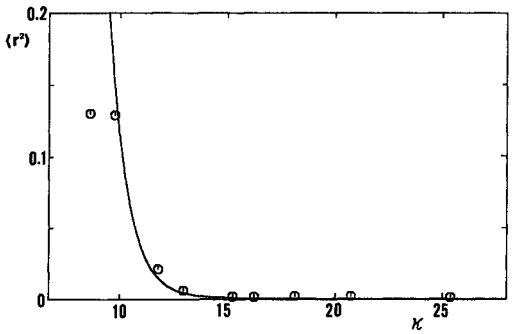

Fig. 6. The averaged value $\langle r^2 \rangle$ in the experiment. The meanings of the circles and the full line are the same as in Fig. 5.

$$\eta = -A(\kappa - \kappa_0) \tag{3·4}$$

with the fitting parameters $A=0.3$ and $\kappa_0=7.0$. The definition of the absolute value r in this section is slightly different from that in § 2. However, similar discussion as in § 2 can be done for the present r and the conclusion obtained in the previous section does not alter.

The averaged values $\langle r \rangle$ and $\langle r^2 \rangle$ are displayed in Figs. 5 and 6, respectively. In order to obtain the averaged values 40000 data points are used with the sampling time interval 20/400 μs for $\kappa=9.75$ and 8.59, and 5/400 μs for $\kappa=11.76 \sim 25.38$. For small κ long-sampling data are necessary because of strong intermittent behavior. The curves in Figs. 5 and 6 are the theoretical ones given in (2·18) and (2·19), respectively, with the fitting parameters, $r_c=5.0$ V and $\varepsilon=0.003$, where the form of the exponent (3·4) is used, since near the intermittent threshold which is defined through $\lambda_m=0$ the linear dependence of the η on the value $(\kappa-\kappa_0)$ may be reasonable.

Consequently, the present intermittency is well understood in terms of the multiplicative noise model presented in § 2. As the exponent η which is proportional to the λ_m approaches zero, the intermittent behavior becomes strong. In the present experiment the region of the positive λ_m or the positive η cannot be found. The positive λ_m region may exist below the lowest value of κ where the experiment has been done.

§ 4. Numerical calculation

In the present section we study the electronic circuit by numerically calculating the basic equations (3·1) with the observed nonlinear characteristics of diodes. The detailed method is given in Ref. 10) and is not described here again. In the real electronic circuit considered in the last section the two diodes have slightly different characteristics. In order to take into account this difference, the nonlinear characteristics of diodes for the forward direction are slightly modified. The voltages across the diodes are written as

$$v_k = V_{Dk}\{\exp(\beta q_k)-1\}, \qquad (k=1, 2) \tag{4·1}$$

where q_k are the reduced quantities corresponding to the charges in diodes. In the present calculation the constants V_{D1} and V_{D2} are taken as 0.7551 and 0.7549, respectively. The parameters in the external field $E(t)$ are put to $V_b=1$ V, $G=5.0$ V and $f=\omega/2\pi=2.75$ MHz. The values of the other parameters are the same as in Ref. 10). The amplitude G in the numerical calculation is chosen so as to get a good qualitative coincidence with the experiment. If one takes the same V_D for both diodes, a uniform state $\Delta V=0$ is realized for the coupling constant κ larger than a certain threshold value.

In Fig. 7 the voltage differences ΔV for different coupling constants are shown. The total time interval for each figure includes 512 periods of the external field ($\sim$186 μs). The strong intermittent behavior is observed as κ is decreased. The power law of the r is also found in the present numerical calculation as is shown in Fig. 8, where $\kappa=11$. In the calculation of the distribution function 4096 data points including 512

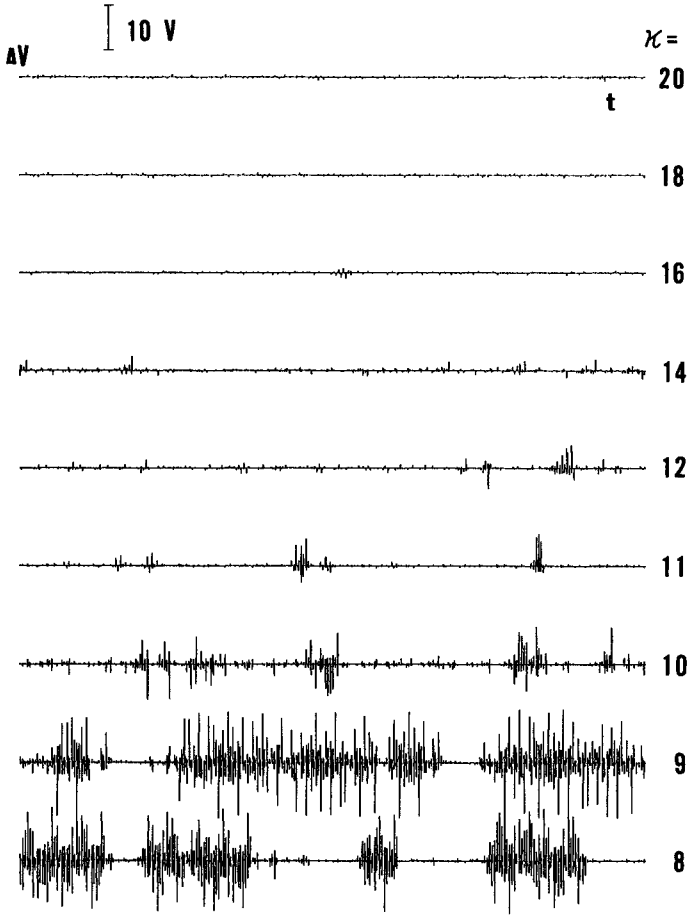

Fig. 7. The same as in Fig. 2 for the numerical calculation.

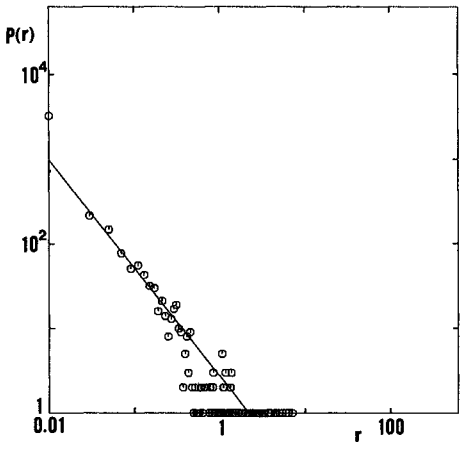

Fig. 8. The same as in Fig. 3 for the numerical calculation.

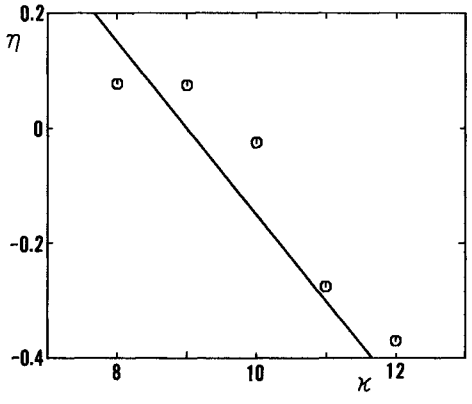

Fig. 9. The same as in Fig. 4 for the numerical calculation.

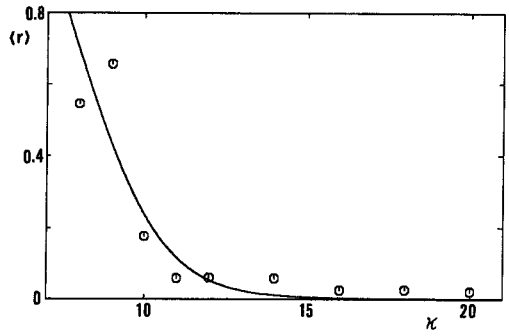

Fig. 10. The same as in Fig. 5 for the numerical calculation.

periods of the external fields are used by digitizing their values in units of 0.02 V. The exponent η is displayed in Fig. 9. The straight line obeys the equation, $\eta = -A(\kappa - \kappa_0)$ with $A=0.15$ and $\kappa_0=9.0$. The exponent η changes the sign near $\kappa \simeq 9$. The calculated averaged value $\langle r \rangle$ is illustrated in Fig. 10. The numerical values are fitted with the theoretical curve where the exponent η is assumed to be written in the form of the straight line in Fig. 9, where the parameters r_c and ε are taken as 4.0 and 0.0001, respectively.

Both in the experiment and the numerical calculation the voltages across diodes are much larger than the voltage difference ΔV shown in Figs. 2 and 7. The voltage difference is sensitive to the choice of the nonlinear characteristics of diodes. Thus, more appropriate set of parameters of the nonlinear characteristics of diodes can exist to fit the results of the numerical calculation with those of the experiment. The present set of the parameters for the numerical calculation is the best among which we have examined.

§ 5. Summary and discussion

We have studied the coupled chaos system in the electronic circuit both experimentally and numerically. The system is realized by connecting two nonlinear LCR circuits with an inductor. Each uncoupled LCR circuit shows chaotic behavior without the coupling through the inductor L_0 in Fig. 1. By decreasing the strength of the coupling constant κ the intermittent behavior can be observed. The present intermittency occurs due to the breaking of the synchronized motion between the chaotic LCR subsystems. The general situation is the same as in the case of type III intermittency.[10]

In the ideal case where two diodes have completely the same characteristics a sharp threshold exists for the transition from the uniform state $\Delta V=0$ to the nonuniform one. However, a small difference of the nonlinear characteristics of two diodes is inevitable in the realistic system. Therefore, in the present work the sharp transition does not appear. This circumstance is analogous to the case of the spontaneous magnetization under external magnetic field in ferromagnetic system. In the present electronic circuit system the difference of the characteristics of two diodes plays the role of the external magnetic field.

The present system consists of two subsystems each of which behaves chaotically. The study of the present system is considered as the first step to the experimental investigation of the spatiotemporal chaos. A technical difficulty exists to make a system with more than two subsystems: Namely, (1) many diodes with similar characteristics should be prepared, (2) a high power supply is necessary. We hope to make a further progress in the experimental study of the spatiotemporal chaos along the

line of the present research.

Acknowledgements

It is a great pleasure for the authors to dedicate the present article to Professor H. Mori on the occasion of his retirement from Kyushu University. One of the authors (T. Y.) would like to express his sincere thanks to Professor H. Mori for permitting him to attend the seminar of the Mori group. In the seminar the author (T. Y.) has always been stimulated in promoting the researches. The authors also thank Professor H. Fujisaka for his valuable discussions.

References

1) P. Manneville and Y. Pomeau, Phys. Lett. **75A** (1979), 1; Physica **1D** (1980), 219.
J. P. Gollub and S. V. Benson, J. Fluid Mech. **100** (1980), 449.
2) H. Fujisaka and T. Yamada, Prog. Theor. Phys. **74** (1985), 918; **75** (1986), 1087.
3) H. Fujisaka and T. Yamada, Prog. Theor. Phys. **69** (1983), 32.
4) T. Yamada and H. Fujisaka, Prog. Theor. Phys. **70** (1983), 1240.
K. Tomita, Prog. Theor. Phys. Suppl. No. 79 (1984), 1.
5) A. Schenzle and H. Brand, Phys. Rev. **A20** (1979), 1628.
6) T. Yamada and H. Fujisaka, Prog. Theor. Phys. **76** (1986), 582.
H. Fujisaka, H. Ishii, M. Inoue and T. Yamada, Prog. Theor. Phys. **76** (1986), 1198.
7) J. P. Crutchfield and K. Kaneko, "Phenomenology of Spatiotemporal Chaos", in *Directions in Chaos* (World Scientific, 1987).
8) P. S. Linsay, Phys. Rev. Lett. **47** (1981), 1349.
9) J. Y. Huang and J. J. Kim, Phys. Rev. **A36** (1987), 1495.
10) K. Fukushima and T. Yamada, J. Phys. Soc. Jpn. **57** (1988), 4055.
11) Z. Su, R. W. Rollins and E. R. Hunt, Phys. Rev. **A36** (1987), 3515.
12) P. Grassberger and I. Procaccia, Physica **13D** (1984), 34.
13) T. Yamada and H. Fujisaka, Phys. Lett. **A124** (1987), 421.